

A STUDY OF FATIGUE BEHAVIOUR OF MODE I  
CRACKS UNDER BIAXIAL LOADING

Yi-Min Yang and Ming-O Wang

Department of Chemical Machinery  
Nanjing Institute of Chemical Technology  
Nanjing, Jiangsu, 210009, People's Republic of China

Third International Conference on Biaxial/Multiaxial  
Fatigue, April 3-6, 1989 Stuttgart, FRG

ABSTRACT

Fatigue tests have been performed on a low carbon alloy steel (Chinese Industrial Standard 16MnR) in a closed-loop servohydraulic biaxial fatigue testing machine. Based on finite element analyses and strain gauge measurements, a reasonable configuration of the cruciform specimen is determined. The Mode I stress intensity factors,  $K_{I}$ , of the central penetrated cracked cruciform specimen with various crack lengths are computed by the contour integral method combined with the finite element analysis. It is found that the value of Mode I stress intensity factor of a cruciform component with a central penetrated crack decreases with the increase of the tension load parallel to the plane of the crack.

The experimental results indicate that when the biaxial load ratio,  $\Lambda = P_x/P_y$ , is greater than zero and the range of Mode I stress intensity factor ( $\Delta K_{I}$ ) is in the scope of 28-70  $\text{MPa}\sqrt{\text{m}}$ , the biaxial load ratio and the rolling direction of the steel plate are of no significance in the relation of fatigue crack growth rate and  $\Delta K_{I}$ .

KEYWORDS

Biaxial loading, fatigue behaviour, Mode I stress intensity factor.

NOMENCLATURE

$\Lambda$  Biaxial load ratio

- $\lambda$  Biaxial stress ratio ( $\lambda = \sigma_x / \sigma_y$ )
- a Half crack length
- $K_I$  Mode I stress intensity factor
- $\Delta K_I$  Range of Mode I stress intensity factor
- E Young's Modulus
- R  $P_{\min} / P_{\max}$

## INTRODUCTION

Structural components are usually subjected to biaxial or multiaxial cyclic loadings. The behaviour of materials in biaxial stress states has been studied for many years. However, there are some discrepancies in the researchers' opinions about the effect of  $\lambda$  on fatigue crack growth rate (FCGR) of Mode I cracks. Truchon<sup>[1]</sup> indicated that the  $\lambda$  has no influence on the FCGR. Gao Hua<sup>[2]</sup> reported that the FCGR decreases with the increase of  $\lambda$ . And Kitagawa<sup>[3]</sup> found that the significant effect of  $\lambda$  on FCGR appears when a crack is small and stress level is high.

Reasons for aforesaid discrepancies might be that the configuration of the biaxial specimens used by the aforementioned researchers are different and the methods of the  $K_I$  calibration for their specimens are not the same. Therefore, in the present paper, a reasonable cruciform specimen was determined. Then, the  $K_I$  values of the specimens used were computed accurately by the contour integral method combined with the elastic finite element analysis. The fatigue tests were conducted on a low carbon alloy steel 16MnR which is widely used in the manufacture of pressure vessels in China under biaxial loading at room temperature and atmosphere. And the effect of the load parallel to the plane of the crack on FCGR has been discussed.

## GEOMETRY OF THE CRUCIFORM SPECIMEN

The cruciform specimen was designed based upon the principle of an uniform stress field in the working region of the cruciform specimen and of a small difference between  $\lambda$  and  $\Lambda$ . By reference to the literatures<sup>[1],[2],[3]</sup>, especially to the literature<sup>[7]</sup>, and upon the results of finite element analyses and strain gauge measurements, the geometry of the cruciform specimen was determined, as shown in Fig.1.

The specimen used in uniaxial fatigue tests for the contrast purpose is depicted in Fig.2.

The stress distributions in the working regions of the cruciform specimens used in the present paper and used in Reference<sup>[3]</sup> are shown in Figs. 4 and 5, res-

pectively. And the stress distribution of the cracked plate subjected to biaxial uniform stresses is shown in Fig.6. The definition of  $\sigma_{x_0}$  and  $\sigma_{y_0}$  is shown in Fig.5. Comparing Fig.4 with Fig.5 and Fig.6, it is found that the configuration of the cruciform specimen used in the present paper is reasonable.

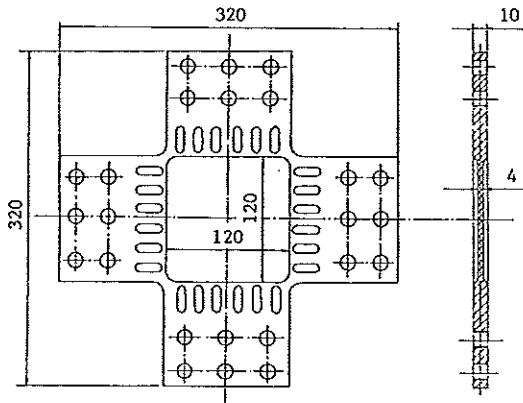


Fig.1 Cruciform specimen  
( all dimensions in mm ).

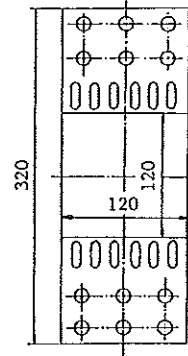


Fig.2 Uniaxial specimen  
( all dimensions in mm )

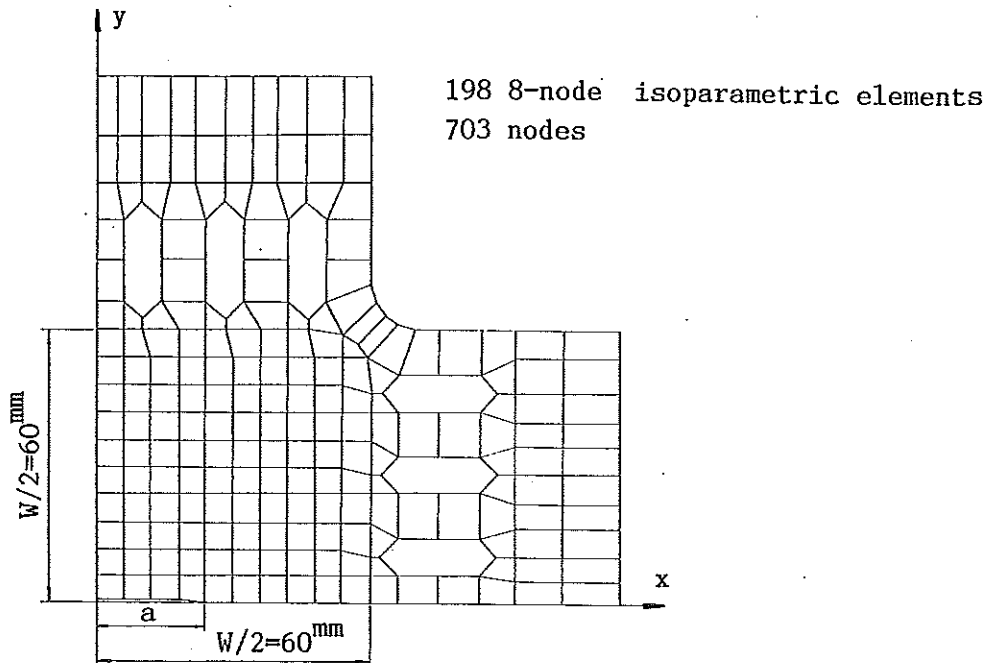


Fig.3 The finite element mesh of one quadrant of the cruciform specimen for the elastic finite element analysis and the  $K_I$  calibration.

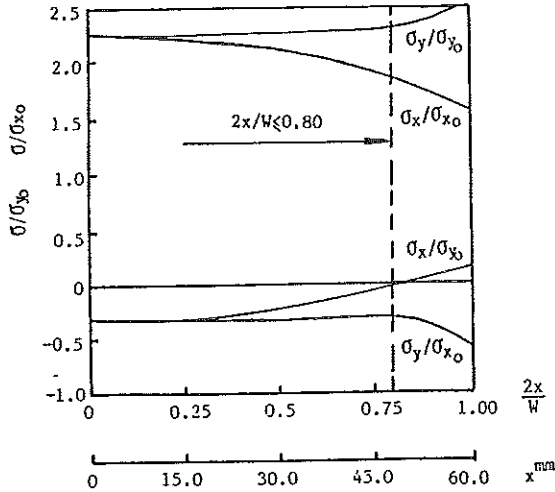


Fig.4 Stress distribution without any crack along the x-axis in the cruciform specimen used in the present paper.

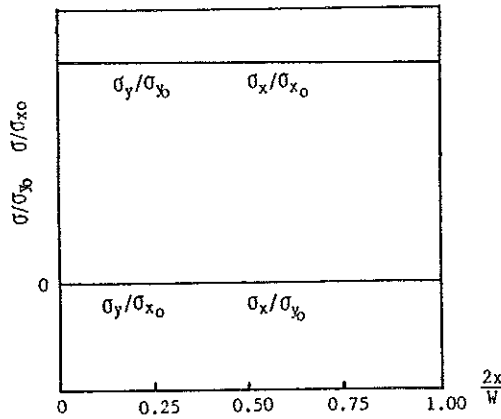


Fig.6 Stress distribution without any crack along the x-axis in the cracked plate subjected to biaxial uniform stresses.

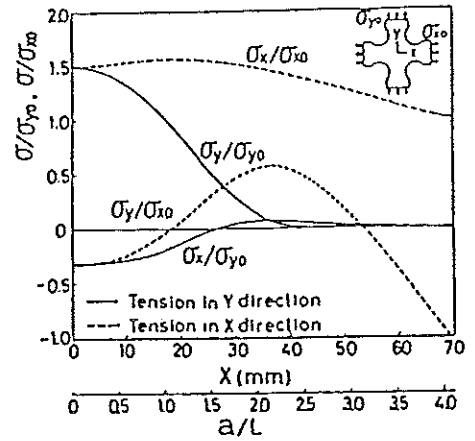


Fig.5 Stress distribution without any crack along the x-axis in the cruciform specimen used in Reference [3].

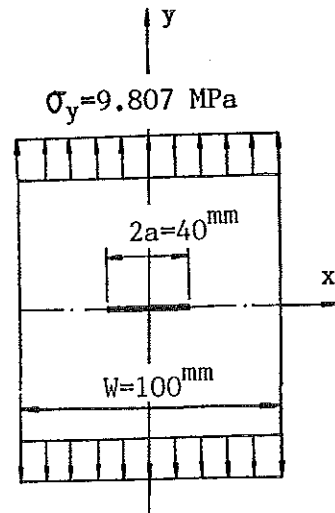


Fig.7 Central cracked plate subjected to uniaxial stresses.

CALIBRATION OF STRESS INTENSITY FACTORS

In the present paper, the  $K_I$  values of the specimens were computed by the contour integral method combined with the finite element analysis. The  $K_I$  for plane stress is given by the following equation [4]

$$K_I = \sqrt{JE} \tag{1}$$

where J can be represented by the equation [5]

$$J = \int_{\Gamma} (W - \sigma_x \epsilon_x - \tau_{xy} \frac{\partial u_x}{\partial x}) dy + (\tau_{xy} \epsilon_x + \sigma_y \frac{\partial u_x}{\partial x}) dx \tag{2}$$

where J = value of J integral,

$\Gamma$  = path of J integral,

W = strain energy,

$\sigma_x, \sigma_y, \tau_{xy}$  = normal and shearing stresses,

$\epsilon_x$  = normal strain in x-axis,  $\frac{\partial u_x}{\partial x}$  = partial derivative.

Firstly, based on eq 2, the J value of the plate containing a Mode I crack

was computed by a method of numerical contour integral while a finite element analysis have been completed. Secondly, the  $K_I$  value was obtained by using eq.1. According to the foregoing procedure, the program FJKP computing the  $K_I$  value was written for a personal computer.

The quarter-point quadratic isoparametric elements were used in the region of a crack tip, and the standard quadratic isoparametric elements were used in the rest region.

As for the cracked plate subjected to uniaxial stresses as shown in Fig.7,  $K_{I \text{ uniaxial}}^{\text{ASTM}}$  (the  $K_I$  obtained by the  $K_I$  calibration given in ASTM Method E647) is equal to  $2.73305 \text{ MPa}\sqrt{\text{m}}$ , and  $K_{I \text{ uniaxial}}^{\text{FJKP}}$  (the  $K_I$  obtained by the program FJKP) is equal to  $2.71678 \text{ MPa}\sqrt{\text{m}}$ . The relative difference between  $K_{I \text{ uniaxial}}^{\text{ASTM}}$  and  $K_{I \text{ uniaxial}}^{\text{FJKP}}$  is equal to 0.599%. Therefore, the accuracy of the program FJKP is high.

As to the cracked plate subjected to equibiaxial stresses, as shown in Fig.8,  $K_{I \text{ equibiaxial}}^{\text{FJKP}}$  (the  $K_I$  value obtained by the program FJKP) is equal to  $2.70725 \text{ MPa}\sqrt{\text{m}}$ . By comparing the values of  $K_{I \text{ uniaxial}}^{\text{FJKP}}$  and  $K_{I \text{ equibiaxial}}^{\text{FJKP}}$ , it is found that the  $K_I$  value of a square plate containing a central crack subjected to biaxial stresses is independent of the biaxial load ratio,  $\lambda$ . The similar conclusion was also obtained in Reference [6].

The finite element mesh for the  $K_I$  computation of the cruciform specimen used in the present paper is shown in Fig.3. Using the program FJKP, the  $K_I$  values of the specimens as shown in Figs. 1 and 2 respectively were obtained, the results are shown in Fig.9 and represented by the equation

$$K_I = F_1 \sqrt{a \sec(F_2 a)} \quad (3)$$

where the constants  $F_1$  and  $F_2$  are listed in Table 1.  $K_I = \text{MPa}\sqrt{\text{m}}$ .  $a = \text{cm}$ .

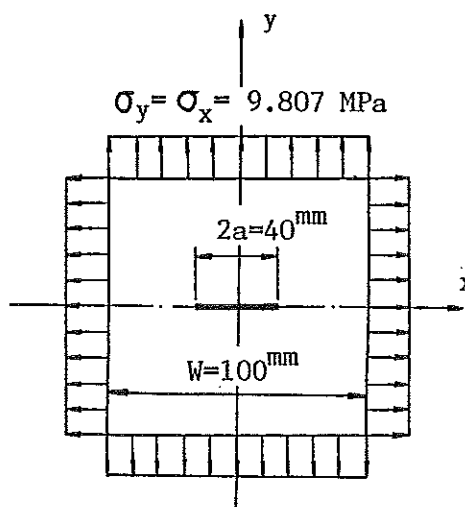


Fig.8 Central cracked plate subjected to equibiaxial stresses.

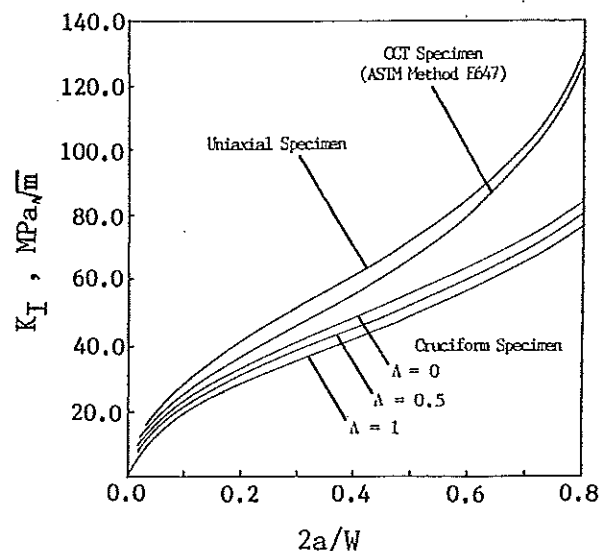


Fig.9 Stress intensity factors for Mode I cracks in the cruciform specimen and the uniaxial specimen.

Table 1 — Coefficients  $F_1$  and  $F_2$  in eq 3

		$F_1$	$F_2$
Cruciform Specimen	0	29.9532	0.189151
	0.5	27.8522	0.197903
	1	25.6537	0.207096
Uniaxial Specimen	0	36.1146	0.249521

As to the cruciform specimen as shown in Fig.1, when  $a$  is equal to  $24^{\text{mm}}$ , according to eq 3

$$\frac{K_I^{\Lambda=0} - K_I^{\Lambda=1}}{K_I^{\Lambda=1}} 100\% = 13.11\%$$

As to the cruciform specimen used in Reference [3], when  $a$  is equal to  $24^{\text{mm}}$ ,

$$\frac{K_I^{\Lambda=0} - K_I^{\Lambda=1}}{K_I^{\Lambda=1}} 100\% = 20.15\%$$

Therefore, the aforesaid analysis shows that the  $K_I$  values of cruciform components are reduced with the increase of the tension load parallel to the plane of the crack.

#### EXPERIMENTAL PROCEDURE

Fatigue crack propagation experiments were carried out on a 16MnR steel. The chemical compositions (wt-%) are C 0.14, Mn 1.46, Si 0.47, S 0.010, and P 0.017. And the mechanical properties are yield strength 375.2 MPa, tensile strength 574.1 MPa, and reduction in area 57.9 %.

All tests were conducted under load control in the closed-loop servohydraulic biaxial fatigue testing machine in a room temperature and atmosphere, using the specimens as shown in Figs. 1 and 2. The frequency of cyclic load is 10 Hz, and the wave form is sinusoidal. The phase difference between the loads of both axes was zero, and the load ratio,  $R$ , employed was 0.05. The experimental conditions of all the five groups of tests conducted in the present paper are listed in Table 2.

At the center of a specimen, a slot of  $8^{\text{mm}}$  length was formed by spark erosion and a pre-formed crack was propagated by fatigue to about  $10^{\text{mm}}$  under uniaxial loading. The crack length was monitored using a travelling microscope.

#### EXPERIMENTAL RESULTS AND DISCUSSIONS

FCGR were determined by the seven point incremental polynomial technique

Table 2 — Experimental Conditions

Ordinal number of the test group	I	II	III	IV	V
$\Lambda$	0	0.5	0.5	1	0
Crack plane orientation	L-T	L-T	T-L	L-T	L-T
Specimen	Cruciform Specimen				Uniaxial Specimen
$P_{y \max}$	98.1 KN				78.5 KN
$P_{y \min}$	4.9 KN				3.9 KN
Number of the specimen tested in this group	3	4	3	4	2

Note — (i) L-T corresponds to the case that the plane of the crack is perpendicular to the rolling direction, and T-L corresponds to the case that the plane is parallel to the direction.

(ii)  $P_{y \max}$ ,  $P_{y \min}$ ,  $P_{x \max}$ , and  $P_{x \min}$  are the maximum and minimum values of the cyclic loads exerted upon the specimen.

(iii) In the fourth group of tests, the specimens in which the cracks propagated along straight paths are listed in Table 2, and other three pieces of specimens in which the cracks propagated along S-shaped paths are not listed in Table 2.

recommended by ASTM Method E647-81. The data of FCGR for the third group of experiments (See Table 2) were presented in Fig. 10.

The regression equations of FCGR versus the  $\Delta K_I$  for the first, second, third, fourth, and fifth groups of experiments were represented by the eqs 4, 5, 6, 7, and 8, respectively

$$\frac{da}{dN} = 6.6 \times 10^{-9} (\Delta K_I)^{2.84} \quad (4)$$

$$\frac{da}{dN} = 6.3 \times 10^{-9} (\Delta K_I)^{2.84} \quad (5)$$

$$\frac{da}{dN} = 6.6 \times 10^{-9} (\Delta K_I)^{2.84} \quad (6)$$

$$\frac{da}{dN} = 6.7 \times 10^{-9} (\Delta K_I)^{2.84} \quad (7)$$

$$\frac{da}{dN} = 6.7 \times 10^{-9} (\Delta K_I)^{2.84} \quad (8)$$

where  $K_I = \text{MPa}\sqrt{\text{m}}$ ,

$$\frac{da}{dN} = \text{mm/cycle}.$$

In order to compare fatigue crack growth behavior conveniently, the exponent value of eq 7 was taken the same as those of eqs 4, 5, 6, and

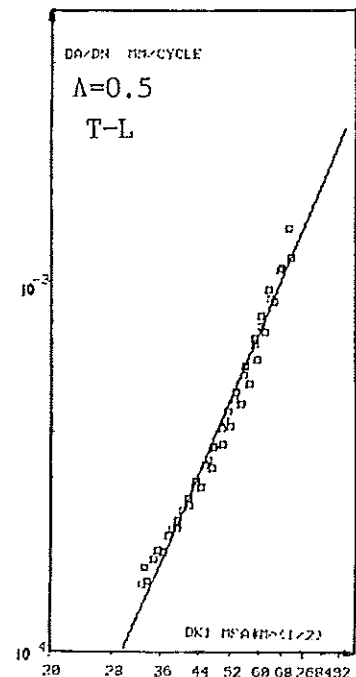


Fig.10 Plot of  $K_I$  versus FCGR for the third group of tests.

8 in regression processing. The upper and lower bounds of the scatter band and the data for all the groups of tests conducted in the present paper are presented in Fig.11. Fig.11 and the eqs 4, 5, 6, 7, and 8 show the  $\Lambda$  and the rolling direction of 16MnR steel have no significant effect on FCGR. And the data for all the groups of tests fall within a narrow band.

The metallographical analysis of 16MnR steel indicates that the microstructure of the material has no apparent directivity. Hence the influence of rolling direction upon FCGR might be negligible. The deduce agrees with the conclusion obtained from fatigue tests. In the equibiaxial fatigue tests, it is found that the crack propagated along an S-shaped path in three pieces of specimens, and in the other four pieces of specimens the crack remained to have propagated along a straight path. These phenomena also were reported by Truchon and co-workers [1].

The reason for the phenomena might be that any direction in the working region of the cruciform specimens is the direction of principal stresses when  $\Lambda=1$  so that the crack growth direction is relatively arbitrary. The reason the conclusion obtained in the present paper on the effect of  $\Lambda$  on FCGR does not agree with the conclusion obtained in Reference [2] is discussed as follows.

Gao [2] reported that the FCGR for uniaxial stress condition is about 30 percent higher than the rate for equibiaxial stress condition. In the other hand, as shown in Fig.11, the conclusion obtained in the present paper is of no apparent effect of  $\Lambda$  on FCGR.

The  $K_I$  value of the cruciform specimen used in Reference [2] is independent of  $\Lambda$ , and the  $K_I$  formula of the cruciform specimen used in the present paper is the

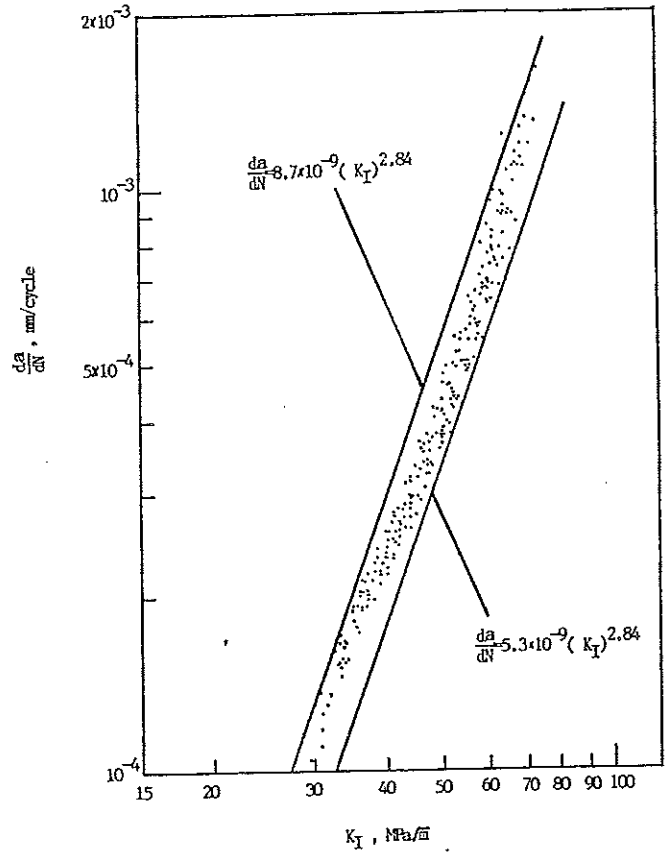


Fig.11 Crack-growth rate as a function of stress-intensity range for all the tests (with the influence of  $\Lambda$  on  $K_I$  having been taken into account).



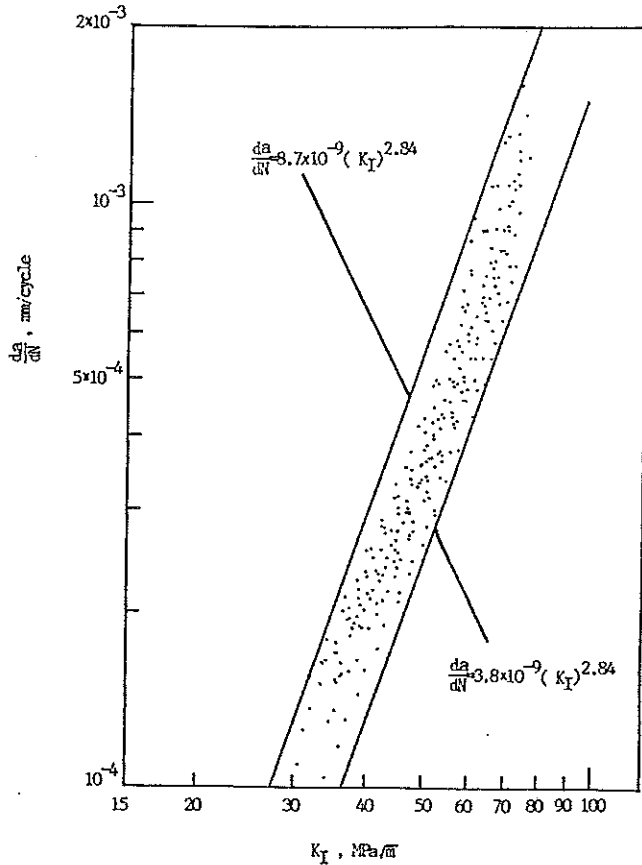


Fig.12 Crack-growth rate as a function of stress-intensity range for all the tests (with the influence of  $\Lambda$  on  $K_I$  not having been taken into account).

function of  $\Lambda$ .

If the influence of  $\Lambda$  on  $K_I$  of the cruciform specimen used in the present paper was disregarded, all the fatigue data were rehandled with the  $K_I$  value for  $\Lambda=0$ , as shown in Figs. 12, and 13. And Fig.13 shows that the FCGR for  $\Lambda=0$  is approximately 30% higher than the rate for  $\Lambda=1$  in the case of neglecting the influence of  $\Lambda$  on  $K_I$  of the cruciform specimen. The result shown in Fig.13 agree roughly with that of Gao in Reference [2] shown in Fig.14.

Thus it seems that the reason the conclusion in the present paper is not consistent with that in Reference [2] might be that the

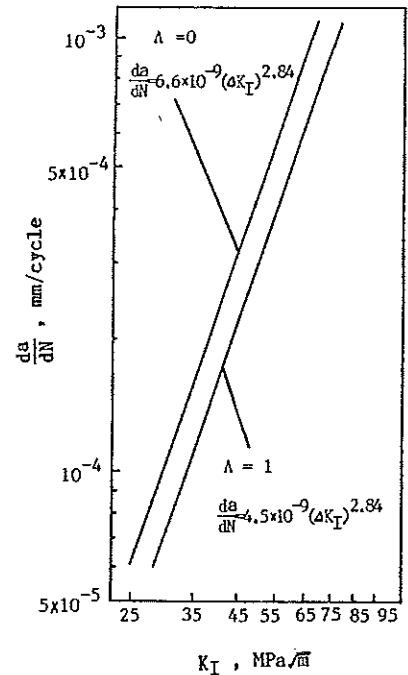


Fig.13 Comparison of FCGR of uniaxial condition with that of equibiaxial condition (with the influence of  $\Lambda$  on  $K_I$  not having been taken into account).

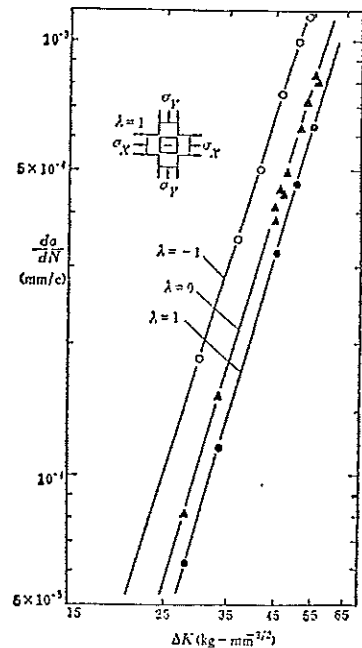


Fig.14 Comparison of FCGR of uniaxial condition with that of equibiaxial condition in Reference [2].

influence of  $\Lambda$  on  $K_I$  for the cruciform specimen used in the Reference [2] was not taken into account in  $K_I$  calibration in Reference [2]. The fatigue data processings of taking and not taking the influence of  $\Lambda$  on  $K_I$  of cruciform specimens into account are presented in Figs.15 and 16, respectively.

By comparing Fig.11 and Fig.12, it is found that the scatter band of data points in Fig.11 is narrower than that in Fig.12. Thus it seems that the influence of  $\Lambda$  on  $K_I$  of cruciform specimens should be taken into account in the processing of biaxial fatigue data.

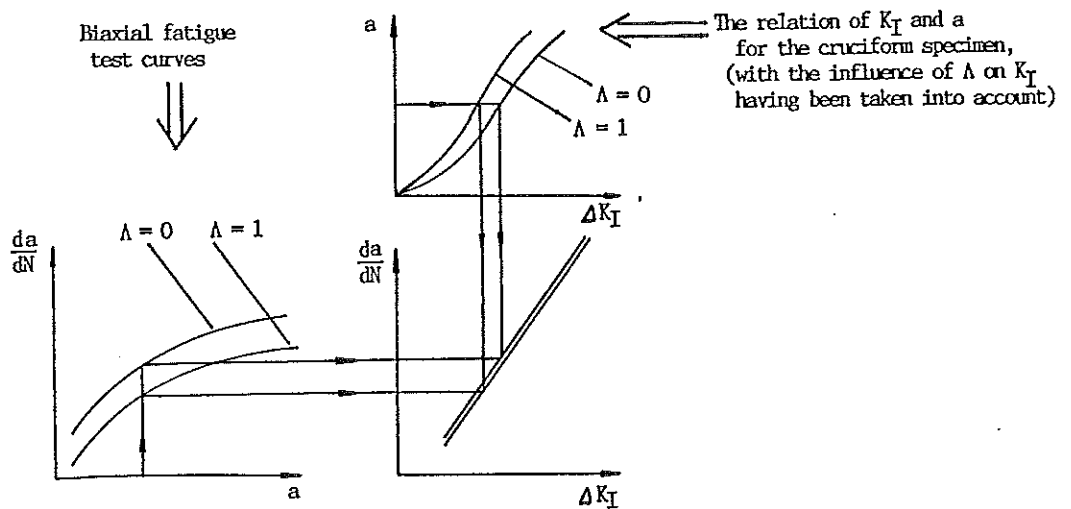


Fig.15 The fatigue data processing of taking the influence of  $\Lambda$  on  $K_I$  of the cruciform into account.

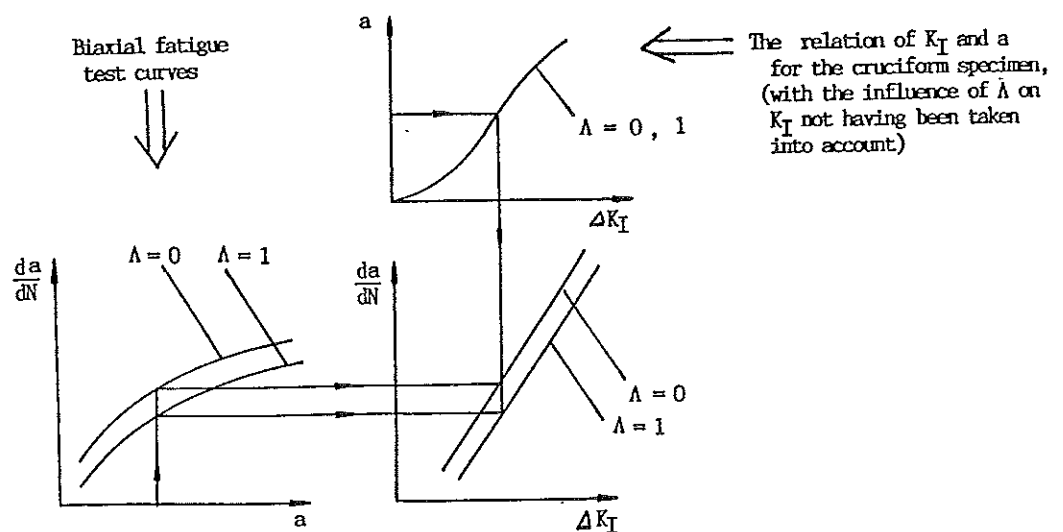


Fig.16 The fatigue data processing of not taking the influence of  $\Lambda$  on  $K_I$  of the cruciform specimen into account.

## CONCLUSIONS

1. The biaxial load ratio and the rolling direction of the steel plate (16MnR) are of no significance in the relation of fatigue crack growth rate and  $\Delta K_I$  when  $\Lambda$  is greater than zero and  $\Delta K_I$  is in the range of 28-70 MPa $\sqrt{m}$ .
2. By using the contour integral method combined with the finite element analysis, it is found that the  $K_I$  values for cruciform-shaped components decrease with the increase of tension load parallel to the plane of the crack.
3. It seems that the reason for the discrepancy between the conclusion on the effect of  $\Lambda$  on FCGR in the present paper and the conclusion in Reference<sup>[2]</sup> might be that the influence of the tension load parallel to the plane of the crack on  $K_I$  value for the cruciform specimen was not taken into account in Reference<sup>[2]</sup>.

## ACKNOWLEDGEMENTS

The authors would like greatly to acknowledge Professor Shu-Ho Dai for his encouragement and many valuable suggestions and guidances in the work of the present paper, and the National Natural Science Foundation Committee of China for financial support for the project.

## REFERENCES

- [1] Truchon, M., Amestoy, M., and Dang-Van, K., Advances in Fracture Research, D. Francois, Eds., Pergamon Press, 1982, Vol.1, pp.1841-1849.
- [2] Gao, H., and Miller, K. J., Acta Mechanica Solida Sinica, December, 1985, pp.151-159, (in Chinese).
- [3] Kitagawa, H., Yuuki, R., Tohgo, K., and Tanabe, M., Multiaxial Fatigue, ASTM STP 853, K. J. Miller and M. W. Brown, Eds., American Society for Testing and Materials, Philadelphia, 1985, pp.164-183.
- [4] Bo-Fang Zhu, The Principle and Application of Finite Element Methods, Hydroelectric Press, 1979, pp.373-393, (in Chinese).
- [5] Rice, J. R., Journal of Applied Mechanics, Vol.35, 1968, pp.379-386.
- [6] Miller, K. J., and Kfoury, A. P., International Journal of Fracture, Vol. 10, No.3, 1974, pp.393-404.
- [7] Brown, M. W., and Miller, K. J., Multiaxial Fatigue, ASTM STP 853, K. J. Miller and M. W. Brown, Eds., American Society for Testing and Materials, Philadelphia, 1985, pp.135-152.